QCM Humidity Sensors Based on Organic/Inorganic Nanocomposites of Water Soluble-Conductive Poly(diphenylamine sulfonic acid)

Şule Dinç Zor[*], *Hüsnü Cankurtaran*

Yıldız Technical University, Faculty of Science and Arts, Department of Chemistry,
34220 Davutpaşa-Istanbul, Turkey
[*]E-mail: sule_dinc@yahoo.com

This paper describes the detection of relative humidity (RH) through measurements of the resonance frequency of the quartz crystal microbalance (QCM) electrodes coated with the novel organic/inorganic hybrid composites of poly (diphenylamine sulfonic acid) (EPSDA), 3-mercaptopropyltrimethoxysilane (MPTMS) and nano-Al_2O_3 powder. EPSDA was synthesized by constant potential electrolysis of diphenylamine sulfonic acid on Pt sheet electrode in HCl media at 0.8 V. The different composite mixtures were simply prepared by ultrasonication of acidic aqueous solution of EPSDA with MPTMS and with or without nano-Al_2O_3. As prepared sol-gels were drop casted onto the quartz electrodes, and then dried to obtain sensing films. The measured frequency shifts under exposure of different humidity levels showed that the whole sensors studied have high sensitivity, durability and repeatability, almost a full range of linear relative humidity response, fast response/recovery times and low hysteresis. Moreover, they have high selectivity towards humidity over the various polar and non-polar solvent vapors such as alcohol, ketone, ester, chlorinated and non-chlorinated hydrocarbons. These results promise that the EPSDA based organic-inorganic hybrid composites have superior properties for relative humidity measurements.

1. INTRODUCTION

Humidity measurements are a very important requirement in industrial processing and environmental monitoring, such as automotive, textile, food processing, agricultural, medical, pharmaceutical and domestic applications [1-3]. The most commonly used units for humidity are

Relative Humidity (RH), Dew/Frost point (D/F PT) and Parts Per Million (ppm). Most humidity sensors are relative humidity sensors [4]. Semiconducting metal oxides, ceramics, organic and inorganic solid electrolytes, insulating and conducting/semi-conducting polymers and various composites have been widely used for sensing humidity and the different gases in industry and research laboratory [5-17]. Metal oxide and inorganic solid polyelectrolyte type of gas sensors have been successfully commercialized for industrial processes and automobile industry, for example [18, 19]. Inorganic semiconducting metal oxides like aluminium oxide (Al_2O_3), tin oxide (SnO_2), iron oxide (Fe_2O_3), zinc oxide (ZnO) and titanium oxide (TiO_2) have been extensively studied to sense humidity as well the other gases. However, metal oxide and ceramic based sensors may suffer from low conductivity and sensitivity at low temperatures and cross response towards reducing and oxidizing gases [4, 20]. Insulating and conducting polymers, polymer electrolytes and their composites with inorganic additives have been studied to progress sensor performance, such as low temperature sensitivity, stability and selectivity [21, 22]. Among them, conductive polymers which may have electronic and/or ionic conductivity showed promising application in sensor technology due to their high conductivity even at low temperatures [23, 24]. The other great advantage of conducting polymer based sensors over other available techniques is that the conducting polymers are more sensitive to small perturbations and their response properties may be improved. Due to their poor mechanical properties and low solubility in common organic solvents, various composites, blends and copolymers of conjugated conducting polymers with other functionalized polymers, inorganic substances and solid polymer electrolytes have been also employed for the amendment of their limited processability [25-29].

Recently, intrinsically conducting polymers which are able to dissolve in water have come into prominence in sensor applications owing to their high self-conductivity, easy processability and environmental stability. Therefore, humidity sensor applications of conducting polymer composites and their hydrophilic sulfonic, carboxylic acid and alkyl ammonium derivatives have been widely studied. [30-32]. In our previous study [33], the water-soluble poly(diphenylamine sulfonic acid) was synthesized chemically (PSDA) and electrochemically (EPSDA). The diblock copolymer of PSDA with polyethylene glycol and the blends of PSDA and EPSDA with a commercial latex of poly(vinylacetate/butylacrylate) (PVAc/BuAcry) were successfully used for almost full range of relative humidity measurements by impedance method [33]. The nanohybrid composite films with 3-mercaptopropyltrimethoxysilane (MPTMS) and nano-ZnO powder were also successively used to enhance the durability of the resistive/capacitive type of humidity sensors of EPSDA in extremely low and high humid conditions [34]. In our studies on the morpohological properties of the EPSDA/MPTMS composites with metal oxide nano powders, the nano-Al_2O_3 composites, in comparison with the ZnO composites, exhibited more uniform structures without cracks. On this account, the nano-Al_2O_3 based composites were considered as convenient materials to prepare quartz crystal microbalance humidity sensors which the uniformity and rigidity of the deposition, in fact, are highly required properties for an efficient and stable transduction of the sensing events [35]. For this purpose, MPTMS and nano alumina (n-Al_2O_3) powder were chosen for matrix modification. It was expected that the polymerized MPTMS might also improve the adhesion properties of the composite to the gold substrate via self-assembling process and fixation of EPSDA into the matrix with the help of

the interactions among EPSDA, Al_2O_3 and silane groups [27, 34-37]. Furthermore, it was hoped that the MPTMS and alumina render novel functionality, higher surface area, rigidity and porosity to improve the humidity selectivity, sensitivity and response kinetic of the EPSDA based sensors previously reported [33, 34].

Among the different transduction method, quartz crystal microbalance (QCM) and surface acoustic wave resonators (SAWs) are versatile, sensitive and powerful methods for monitoring mass changes in nano-gram range and sensing properties of appropriate chemically sensitive materials towards target molecules [38,39]. According to Sauerbrey equation [40], the mass change is directly proportional with the shift (Δf) on the fundamental resonant frequency of the quartz crystal:

$$\Delta f = -[2f_0^2 \Delta m]/[A(\rho_q \mu_q)^{1/2}] \tag{1}$$

where f_0 (Hz) is the natural resonant frequency of the quartz crystal (Hz), Δm is the mass change (g), A is the surface area (cm^2) of the crystal, ρ_q is the density of quartz (2.648 gcm^{-3}) and μ_q is the shear modulus of AT-cut quartz crystal (2.947x10^{11} gcm^{-1}s^{-2}). According to equation 1, for a 5 MHz AT-cut crystal (331 μm thickness), Δf equals to 56.6 Hz for 1 μg mass change on per unit surface area. The Sauerbrey equation is valid if the added mass is a uniformly distributed rigid thin film such as metallic coating, metal oxide, thin adsorbed layer, which does not dissipate any energy during oscillation. [41]. The linear relationship between Δf and Δm in the Sauerbrey equation holds when $\Delta f <$ 0.02f_0. For the 5 MHz crystal used in this study, the theoretical upper limit for the linear range in Sauerbrey equation is 100 kHz. The gold electrodes on the quartz may be easily coated with multifunctional compounds such as thiols by forming surface assembled monolayers (SAMs) via thiol groups [42]. This procedure enhances adhesion properties of the films onto the electrode and affords new opportunities for further modifications. Therefore, QCM method was considered to be a good choice to investigate the humidity sensing properties of the thiol-containing composite films used in this study.

2. EXPERIMENTAL

2.1. Materials

The sodium salt of diphenylamine sulfonic acid and hydrochloric acid were analytical grade Aldrich products. 3-mercaptopropyltrimethoxysilane (MPTMS, purity 95 wt%), nano Al_2O_3 powder (n- Al_2O_3, <50 nm) were supplied by ABCR. LiCl, $Mg(NO_3)_2$, and K_2SO_4 were provided from Merck. The Millipore water had a specific resistance of 18.1 MΩcm. Water (W) and analytical grade of Merck and Aldrich products of ethanol (Eth), acetone (Ace), chloroform (Chl), n-hexane (n-Hex), tetrahydofuran (THF) and n-butylacetate (n-BA) were used to investigate the sensors responses against different solvents.

2.2. Instruments

For electrochemical polymerization of EPSDA, a Radiometer PST050 potentiostat was used. A Pt sheet (2x3 cm), Ag/AgCl (3 M KCl) and Pt wire were employed as working, reference and auxiliary

electrode, respectively. A SRS QCM200 digital controller, a QCM25 crystal oscillator and AT-cut quartz crystals (5 MHz resonant frequency, 56.6 Hz/μgcm^2 sensitivity) were used for mass sensitive sensor experiments. A capacitive type of commercial humidity sensor (Carl Roth P330) which has a 0-99% relative humidity measuring range with an accuracy of $\pm$3%RH was used to measure actual humidity. Its calibration was performed with the saturated salt solutions of LiCl (12%RH), Mg(NO$_3$)$_2$ (55%RH) and K$_2$SO$_4$ (97.6%RH) within the limits of accuracy. Equilibrium response time of the commercial and studied sensors was also observed to be similar in flowing gas atmosphere. An Aalborg SDPROC flow controller and two AFM 26 mass flow meters were used to obtain different humid conditions in flow. Different RH% values were obtained by adjusting the flow rate of the dry and humidified nitrogen. Measurement system is shown in Fig.1. In addition, an ambient air supplied from an air pump instead of pure nitrogen was used to see the effect of the contaminants in the laboratory atmosphere. To compare the response behavior of the sensors towards humidity and solvent vapors, the measurements were carried out in nitrogen atmosphere saturated with the studied solvent vapors. Infrared spectra of the sensing materials were recorded with a Perkin Elmer Spectrum One FT-IR spectrometer. Scanning electron microscope (SEM) images of prepared sensor films were characterized by a Philips XL 30-ESEM-FEG/EDAX instrument.
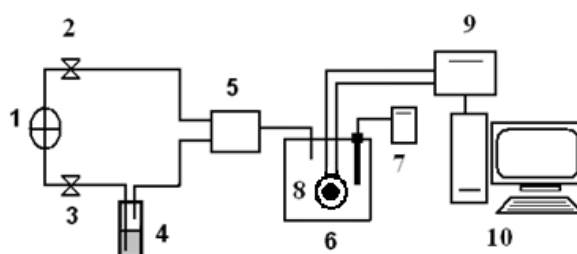
Figure 1. QCM measurement setup: 1) N$_2$ tank, 2, 3) flow control, 4) gas washing bottle, 5) gas mixing chamber, 6) measurement chamber, 7) reference humidity sensor, 8) quartz crystal, 9) QCM frequency counter, 10) computer.

2.3. Preparation of EPSDA/polysilane hybrid composites

Synthesis and characterization of EPSDA were reported in our previous studies and not given here again [33, 34]. Each of 20 μL of 1%, 5% and 10% EPSDA (wt/v%) in 0.1 M HCl were mixed with 5 μL of MPTMS and diluted to 1.0 mL with water. These mixtures ultrasonically agitated for 15 min.
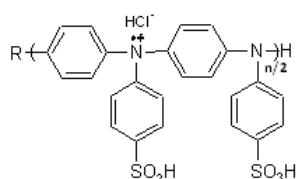
Figure 2. Poly(diphenylamine sulfonic acid).

After sonication, each of 50 µL of the sol-gel was dropped onto the quartz crystal taking care to obtain approximately definite coating surface area on the crystal. The as-prepared films were allowed to dry at room temperature and then cured by oven drying at 105 ^{0}C for 2 h. The molecular structure of EPSDA and the composition of the prepared films are given in Fig. 2 and Table 1, respectively.

Table 1. Film composition of the prepared sensors.

Sensor code	Added EPSDA (wt/v%)/(µL)	MPTMS (µL)	Nano Al_2O_3 (mg)
QE1	5/20	5	-
QE2	1/20	5	-
QE3	10/20	5	-
QE4	5/20	5	4
QE5	5/20	5	12

2.4. Preparation of EPSDA/polysilane/Al$_2$O$_3$ hybrid composites

20 µL of 5% EPSDA in 0.1 M HCl and 5 µL of MPTMS were mixed and diluted to 1.0 mL with water. Next, 4 mg or 12 mg of nano Al_2O_3 was added into the mixture and ultrasonically agitated for 15 min (Table 1). The same casting, drying and curing procedures given above were used to obtain these films.

3. RESULTS AND DISCUSSION

3.1. SEM images of the composite films

Our previous studies on some diblock copolymer and blends of EPSDA showed that the high EPSDA content in some of the composites may causes to the film deformation via cracking in dry or low humid condition [33]. In terms of good mechanical stability of dried films and also their high durability in humid atmosphere, we found that the addition of MPTMS and metal oxide powders improves the properties of EPSDA films against cracking and/or deterioration in such conditions [34].
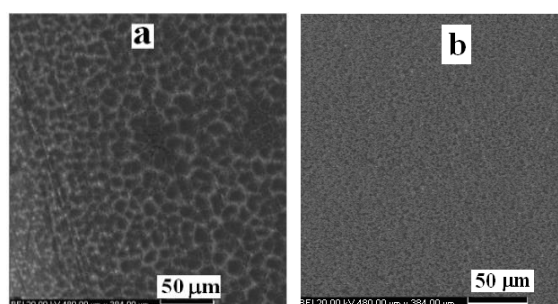
Figure 3. SEM images of a) EPSDA/MPTMS: 80/20 wt%, b) EPSDA/MPTMS/Al$_2$O$_3$: 40/10/50 wt%.

It was also expected that the MPTMS addition enhances the chemical and thermal stability and adhesion properties of the films onto the gold electrode of quartz crystal. In this study, we prepared two SEM samples of EPSDA with polysilane and with or without Al_2O_3: 1) EPSDA/MPTMS: 80/20 wt%, 2) EPSDA/MPTMS/Al_2O_3: 40/10/50 wt%. As shown from the SEM images of EPSDA/polysilane film in Fig. 3.a, EPSDA is uniformly disturbed, like micro-droplets, in the highly ordered polysilane network and no cracks were formed [34]. A highly homogeneous distribution of the film components in the sub-micron porous structure can be observed for the Al_2O_3 added EPSDA/polysilane composite (Fig. 3.b). These results confirm the uniformity and structural stability of the composite films.

3.2. Humidity sensing characteristic of the hybrid composite sensors

The resonant frequency shifts of the film coated quartz crystals were measured between 19 and 59 kHz, as in accordance with the coated mass for QE1, QE2, QE4 and QE5 sensors. However, the resonant frequency of QE3 sensor, which has the highest EPSDA content among the studied films, could not be measured. This indicates great attenuations in acoustic energy, which can be ascribed to the less porous viscoelastic properties of QE3 film.

QE1 sensor exhibits a highly sensitive and repeatable frequency response behavior towards humidity (Fig. 4). The total frequency shift upon repeated cycling exposure of 1%RH and 90%RH was 2699 Hz (RSD= 0.6%). In the similar conditions, resonant frequency shift of an uncoated quartz crystal was only 10 Hz. QE2 sensor did not give a linear response in a reasonable large range of humidity. It has rather low sensitivity at lower humidity ranges, probably due to the low EPSDA content in the composite. On the other side, the frequency readings for QE3 sensor (highest EPSDA content among the studied films) were not stable and repeatable when it was studied in high humid conditions. On these grounds, QE1 sensor was used for further studies to explore sensing performance of EPSDA/polysilane based films.

The study on sensing behavior of nano-Al_2O_3 added composites was conducted on QE4 and QE5 sensors. Similar to the QE1 sensor, they gave highly repeatable frequency responses towards humidity as demonstrated for QE5 sensor in Fig. 5. The total frequency shifts between many exposure cycles of the lowest and highest relative humidities were 3161 Hz (RSD= 0.2%) for QE4 and 22964 Hz (RSD= 0.3%) for QE5 sensor. It is noticeable that while the QE4 sensor (39 wt% Al_2O_3 content) is slightly higher sensitivity than QE1 sensor, QE5 sensor (66 wt% Al_2O_3 content) has much higher sensitivity than the others. By means of frequency shifts correspond to the water uptake and the coated mass on the electrode, it was found that QE4 sensor has a lower water adsorption capacity than that of QE1 sensor. This may be related with the lower EPSDA percentage in the composite film on QE4 sensor. On the other side, it is noteworthy that QE5 sensor (the lowest EPSDA content among the studied sensors), has the highest adsorption capacity. These results indicate that the contribution of hydrophilicity, surface area and porosity of QE1 and QE4 sensors on response results with similar sensitivity but, further increase of nano Al_2O_3 content in the composite facilitates physical adsorption process of water due to the increasing surface area and porosity leading to higher sensitivity of QE5

sensor to water. It is also clear from the frequency shifts that more water molecules may be adsorbed diffusing into the inner side of the bulk film on QE5 sensor. It was considered that high capillary condensation of water would be crucial for higher sensitivity. The quantity of condensed water depends on the open pore size and the RH values [43].

Calculated relative standard deviations in the frequency at the lowest and highest humidity conditions were 0.9%, 0.4% and 0.6% for QE1, QE4 and QE5 sensors, respectively. These results confirm the high repeatability of the studied sensors.

The calibration curves were constructed by plotting the frequency readings towards the relative humidity for QE1 (slope=-31.09 Hz/RH%, R^2=0.9911), QE4 (slope= -35.96 Hz/RH%, R^2=0.9914) and QE5 (slope= -264.79 Hz/RH%, R^2= 0.9950) sensor as shown in Fig. 6. The high linear response characteristics of QE1, QE4 and QE5 sensors in the large humidity ranges can be apparently shown from these results.
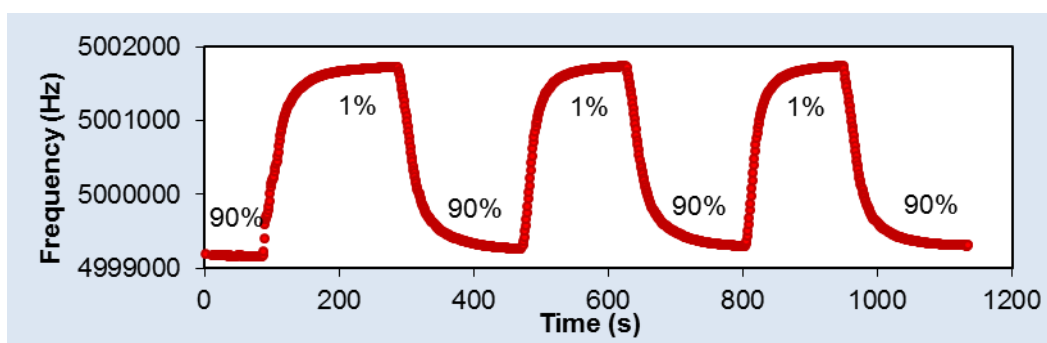
Figure 4. Time dependent changes on the resonance frequency of QE1 sensor upon successive exposure cycles of 1%RH and 90%RH.
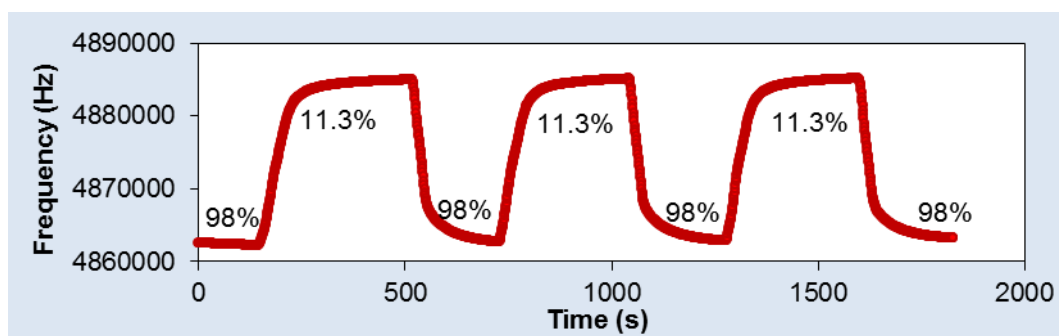
Figure 5. Time dependent changes on the resonance frequency of QE5 sensor upon successive exposure cycles of 11.3%RH and 98%RH.

Another important performance parameter of humidity sensors is hysteresis property which is determined by measuring the steady state sensor signal in successive stepwise hydration/dehydration cycles. It was demonstrated for QE4 sensor in Fig. 7. The calibration plots for QE1, QE4 and QE5 sensors are shown for both stepwise hydration and dehydration cycles in Fig. 8. It is evident that QE1

sensor has higher hysteresis at lower humidity levels (inset in Fig. 8). This is probably related with the nature of adsorption phenomena. It was considered that the sensing mechanism at low humid conditions is mainly based on thermodynamically favored strong chemical adsorption of water on highly hygroscopic EPSDA polymer (it was measured that polysilane film has not a significant humidity response) [44]. Strong interactions are expected among water, free sulfonic acid and HCl doped amine groups [45, 46]. Therefore, it is not surprising that the desorption rate is lower compare to that of sorption resulting low frequency readings in stepwise desorption step. Even so, the calculated hysteresis of QE1 sensor was not more than ±5%RH at low and moderate humidity levels.
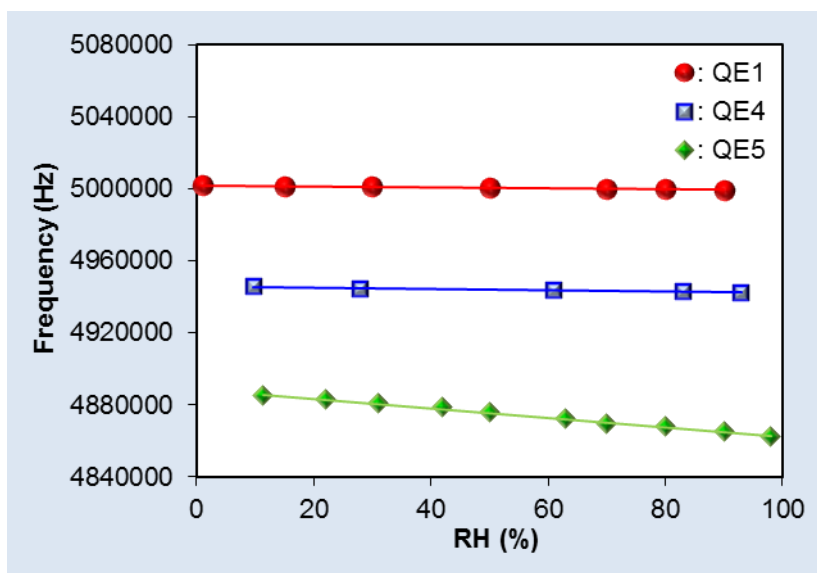

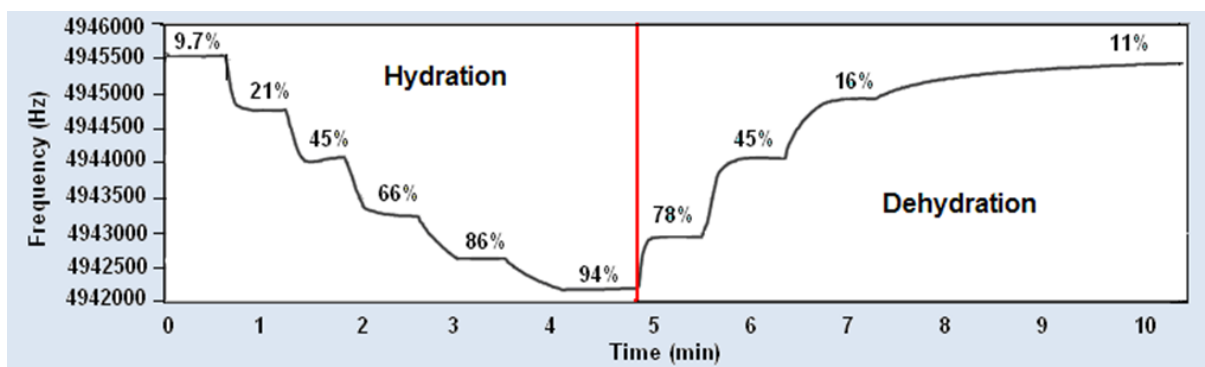**Figure 6.** Calibration curves for QE1, QE4 and QE5 sensors.

Figure 7. Transient frequency responses of QE4 sensor in successive stepwise hydration/dehydration cycles.

The calibration curves of QE4 sensor obtained for stepwise adsorption and desorption process almost overlapped indicating a very small amount of hysteresis for QE4 sensor. In the case of QE5 sensor, the frequency readings during desorption steps are slightly higher than those of humidification,

and the corresponding maximum hysteresis appeared at around 50%RH, was less than ±5.0%RH. This fact demonstrates that the rate of humidification process is slower than that of desiccation. It was considered that both the chemical and physical adsorption processes contribute to the response of EPSDA/polysilane/Al_2O_3 composite films towards humidity. It is expected that the desorption rate of physically adsorbed water molecule should be faster than that of chemically one. It is evident that QE1, QE4 and QE5 sensors have reasonable low hysteresis. The response and recovery times support these behaviors of the sensors. The response and recovery times of the sensors have been measured by adjusting the humidity between lowest and highest levels. The response or recovery time is the time required to achieve 90% of the steady frequency when the humidity is increased and decreased between two levels, respectively. In this study, these levels were close to 1%RH and 90%RH. The response and recovery times were found to be 70 s and 44 s for QE1 sensor, 65 and 45 s for QE4 sensor and 109 and 70 s for QE5 sensor, respectively. It is worth noting again here that, although QE5 sensor has a higher sensitivity than QE1 and QE4 sensors, it has relatively higher response and recovery times. Because, more time are required for the adsorption and desorption of higher amount of water in thicker films. It must be noticed that the film thickness increases in the order of QE1<QE4<QE5. As shown for QE4 sensor in Fig. 7, the response and recovery times could be shorter than these values if the narrower changes in humidity levels were chosen in these experiments. Also, it is obvious in Fig. 7 that the response time at high humidity levels, and recovery time at low humidity levels is getting increase.
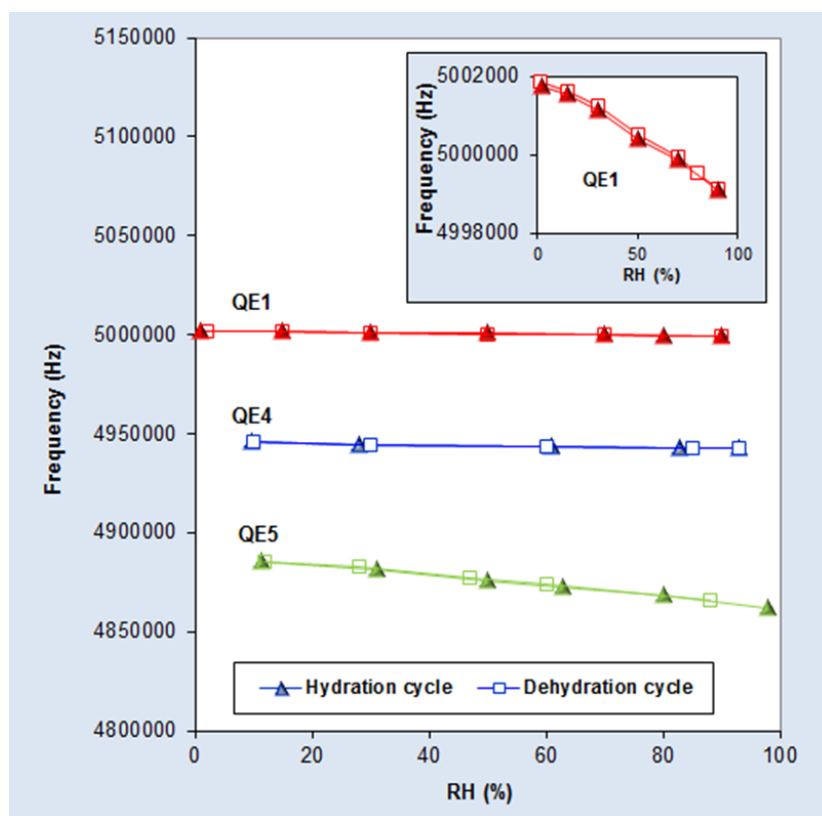
Figure 8. Hysteresis loops of frequency measured by repeated hydration/dehydration cycles for QE1, QE4 and QE5 sensors. The inset shows hysteresis loop of QE1 sensor in enlarged scale.

3.3. The nature of water transport process

The most commonly used method to characterize the nature of the transport process is to fit the initial portion of the sorption curve with

$$M_t/M_\infty = kt^\alpha \tag{2}$$

Where M_t is the mass of vapor sorbed at time t and M_∞ that at complete equilibrium; k is a parameter that depends on the structural characteristics of the material and its interaction with penetrant molecules. For a flat sheet, anomalous diffusion is indicated by $0.5 < \alpha < 1$; while $\alpha = 0.5$ corresponds to Fickian diffusion [47].

To understand the nature of the water diffusion in the sensors, we fit the Eq. (2) to our experimental data in the sorption cycle of humidity between dry and saturated humid atmosphere. Since the frequency shift is linearly proportional with the mass change, M_t and M_∞ were replaced with ΔF_t and ΔF_∞ in Eq. (2) and calculated from the frequency shift at time t and equilibrium, respectively. These two parameters can be given as follows:

$$\Delta f_t = f_0 - f_t \text{ and } \Delta f_\infty = f_0 - f_\infty \tag{3}$$

where, f_t is the frequency during the adsorption process at time t, f_∞ is the frequency in the equilibrium state and f_0 is the initial frequency of the film.

Fig. 9 displays the plots of $\Delta F_t/\Delta F_\infty$ versus $t^{0.5}$ for QE1, QE4 and QE5 sensors. The good linear correlations ($R^2 > 0.9924$) were found suggesting the Fickian diffusional humidity sensing and monotonic sorption behavior of the sensors up to about 70% of the full response.
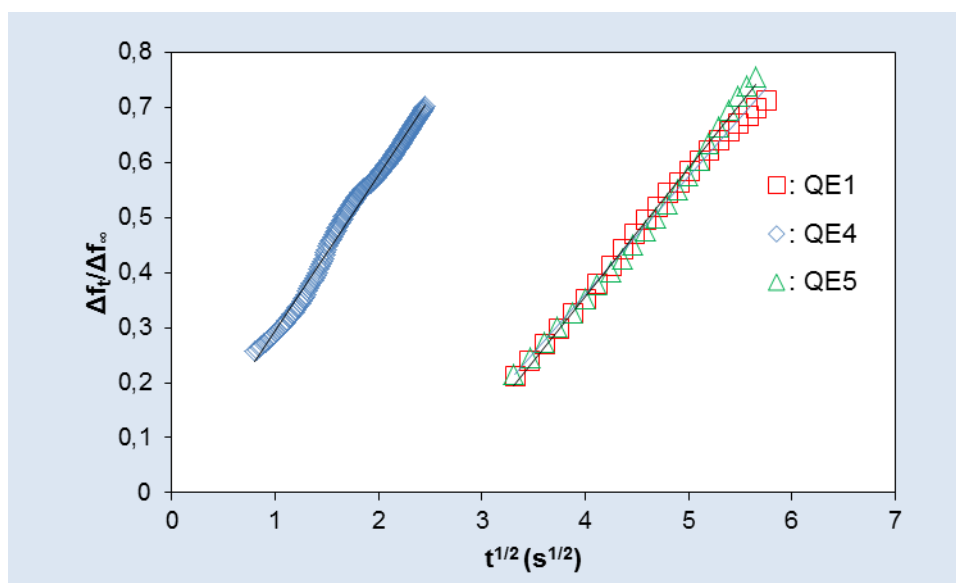

Figure 9. Kinetics of mass uptake for QE1, QE4 and QE5 sensors.

3.4. Stability and long-life durability of the sensors

The results given above showed that the whole sensors have high repeatability under repetitive measurements in extreme conditions. The hysteria studies supported these results. In order to study the long-life durability of the sensors, three resonance frequency readings at the same humidity level were

recorded periodically during thirty days of time lag. QE1 and QE5 sensor were chosen as models and these measurements were repeated for different humidity levels (Fig. 10). It must be noted that these sensors were used continuously for tens of measurements under different humid atmospheres between these periods. It can be concluded that the sensors have high repeatable responses even after thirty days. Additionally, these sensors were washed with water to test their stability under condensed or liquid phase of water.
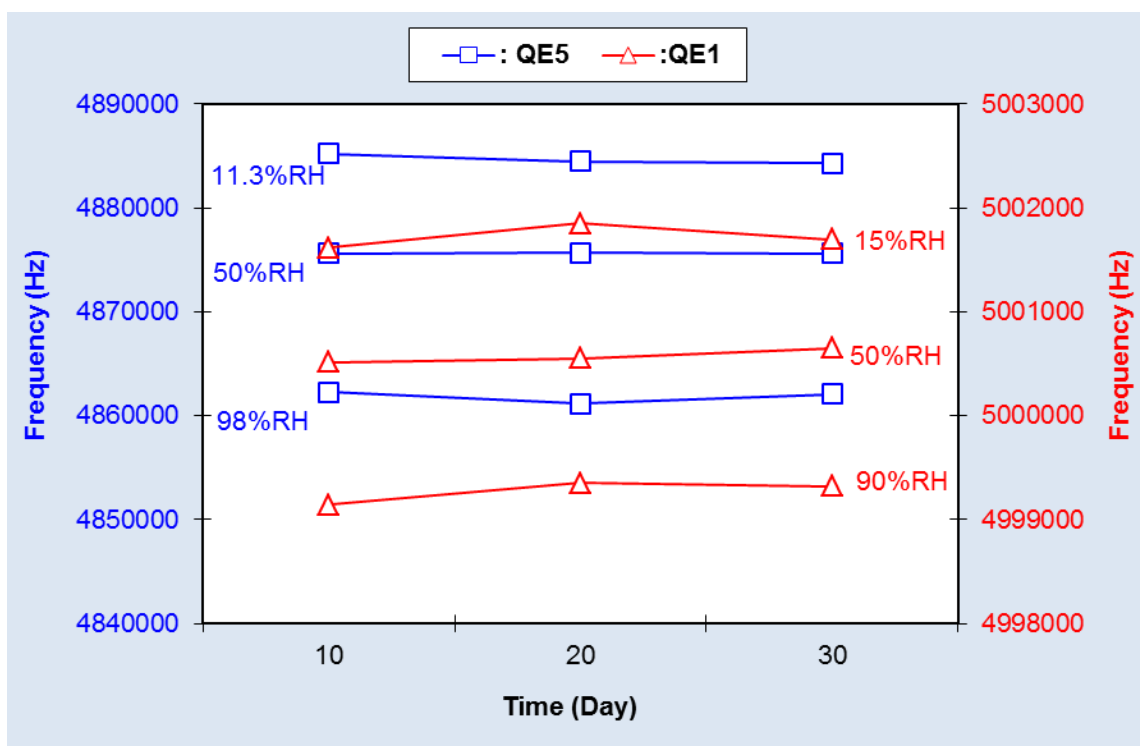

Figure 10. Long-life durability test of the QE1 and QE5 sensors.

It was observed that some EPSDA was stripped from QE1 film to the water and the sensitivity of QE1 sensor was slightly changed. It could be used again but needs to a new calibration procedure. Fortunately, no deterioration was observed for QE4 and QE5 sensors in the same conditions and their response properties were not significantly changed. This is probably due to the strong interactions between the film components enhancing with the presence of Al_2O_3 [27, 36, 37]. Interactions between weak acidic thiol groups on polysilane and deprotonated basic amine groups on EPSDA should also be taken into account [48]. Furthermore, it can be expected that the durability of the sensing films increases due to the bond formation between the free thiol groups and Au surface. The IR band at 1176 cm^{-1} which belongs to the symmetric vibration of free –S=O group of EPSDA disappeared in EPSDA/MPTS/Al_2O_3 composite film and a new peak was existed at 1217 cm^{-1}. In addition, the band at 1370 cm^{-1} which belongs to the asymmetric vibration of free –S=O group of EPSDA shifted to 1366 cm^{-1} in higher intensity. These results clearly indicate the interactions among EPSDA, Al_2O_3 and polysilane in the composite film.

3.5. Selectivity of the sensors

One of the most crucial properties of sensors is the selectivity towards target analyte. In this study, we studied the response behavior of the sensors against various types of solvent vapors. This behavior was demonstrated for QE1 and QE4 sensors by measuring the frequency shifts under saturated vapor atmosphere of solvents. As shown from Fig. 11, both EPSDA/MPTMS and EPSDA/MPTMS/Al_2O_3 based sensors exhibit similar and extremely high selectivity towards humidity. It is obvious that the saturated vapor pressure of the solvents is not a determining factor on the relative sensor responses. On the other side, more polar solvents caused to the higher frequency shifts. It must be due to the high solubility of EPSDA in water. EPSDA was not soluble in common solvents such as saturate hydrocarbons, halogenated hydrocarbons, alcohols, ketones, ethers and esters. In addition, there was no obvious difference in sensor responses under the normal air conditions. Consequently, the sensor response does not be influenced from atmospheric oxygen, minor components and pollutants of air such as CO_2 and SO_2.
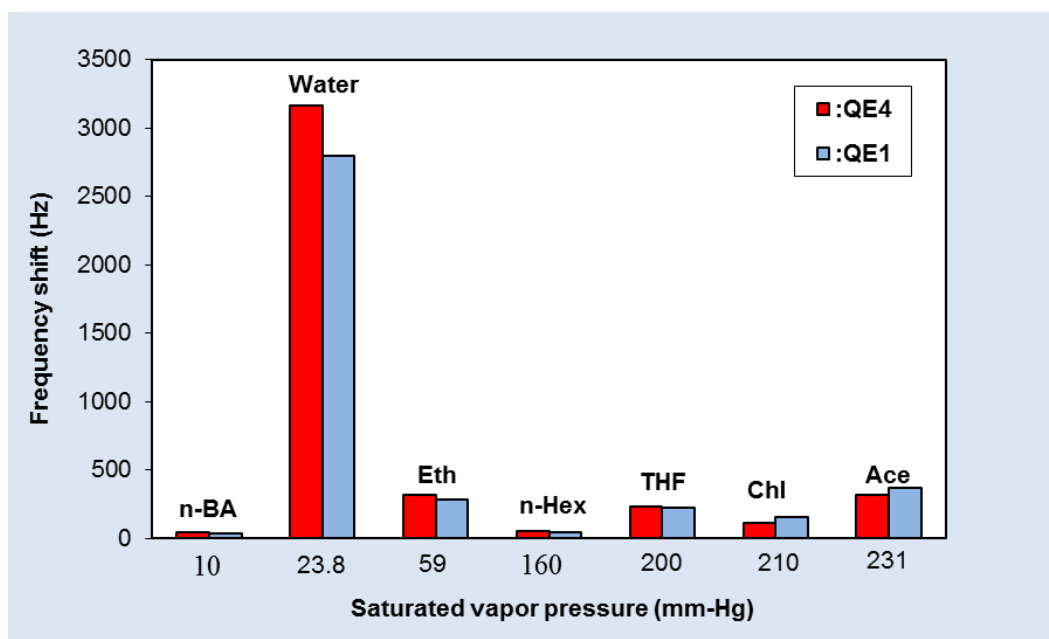
Figure 11. Frequency shifts of QE1 and QE4 sensors under saturated vapor atmosphere of solvents.

4. CONCLUSION

In this study, novel EPSDA/polysilane composite films with and without nano-alumina were used as sensitive elements for relative humidity measurements by QCM method. EPSDA/polysilane based films exhibited higher humidity sensitivity as compared with insignificant sensitivity of polysilane based films in almost full relative humidity range. Composite film of EPSDA/polysilane made of 69% Al_2O_3 showed highest sensitivity. The results supported that both chemical and physical adsorption of water contribute to the total frequency shift. The presence of thiol functionalized

polysilane and nano-alumina in the EPSDA based films improved the stability of the films, and generated high repeatability, sensitivity and large linear dynamic range of sensor responses towards humidity. It can be concluded that EPSDA was fixed into the polysilane/Al_2O_3 network. In addition, the studied composite films have low hysteresis, fast response/recovery time and high selectivity towards humidity over various polar and non-polar solvent vapors. Water solubility and electrical conductivity of PSDA offer great advantages for preparing conductive composite blends with other type of humidity sensitive materials by sol-gel method in aqueous solutions.

References

1. N. Yamazoe, Y. Shimizu, *Sensor Actuators* 10 (1986) 379–398.
2. E. Traversa, *Sens Actuators B Chem*. 23 (1995) 135-156.
3. H. Farahani , R. Wagiran, M. N. Hamidon, *Sensors* 14 (2014) 7881-7939.
4. Z. Chen, C. Lu, *Sensor Letters* 3 (2005) 274-295.
5. M. Li, X.L. Chen, D.F. Zhang, W.Y. Wang, W.J. Wang, *Sens Actuators B Chem*. 147 (2010) 447-452.
6. M. Bayhan, N. Kavasoglu, *Sens Actuators B Chem*. 117 (2006) 261-265.
7. N. Van Quy, V.A. Minh, N. Van Luan, V.N. Hung, N. Van Hieu, *Sens Actuators B Chem*. 153 (2011) 188-193.
8. S.W. Lee, N. Takahara, S. Korposh, D.H. Yang, K. Toko, T. Kunltake, *Anal Chem*. 82 (2010) 2228-2236.
9. P.G. Su, W.C. Li, J.Y. Tseng, C.J. Ho, *Sens Actuators B Chem*. 153 (2011) 29-36.
10. T. Fei, K. Jiang, S. Liu, T. Zhang, *Sens Actuators B Chem*. 190 (2014) 523–528.
11. V. K. Tomer, S. Duhan, *Appl. Phys. Lett.* 106 (2015) 063105.
12. K.P. Yoo, L.T. Lima, N.K. Mina, M.J. Lee, C.J. Lee, C.W. Park, *Sens Actuators B Chem*. 145 (2010) 120-125.
13. A.Vijayan, M. Fuke, R. Hawaldar, M. Kulkarni, D. Amalnerkar, R.C. Aiyer, *Sens Actuators* B Chem. 129 (2008) 106-112.
14. M.M. Ayad, N.L. Torad, *Sens Actuators B Chem*. 147 (2010) 481–487.
15. T. Fei, H. Zhao, K. Jiang, T. Zhang , *Sens Actuators B Chem*. 208 (2015) 277–282.
16. Y.D. Park, B. Kang, H. S. Lim, K. Cho, M. S. Kang, J. H. Cho, *Appl. Mater. Interfaces*, 5 (2013), 8591–8596.
17. W.Geng, X. He, Y. Su, J. Dang, J. Gu, W. Tian, Q. Zhang, *Sens Actuators B Chem*. 226 (2016) 471-477.
18. N. Yamazoe, *Sens Actuators B Chem*. 108 (2005) 2-14.
19. K. Arshak, E. Moore, G.M. Lyons, J. Harris and S. Clifford, *Sensor Review* 24, 2 (2004) 181-198.
20. S.M. Kanan, O.M. El-Kadri, I.A. Abu-Yousef, M.C. Kanan, *Sensors* 9 (2009) 8158-8196.
21. B. Adhikari, S. Majumdar, *Prog Polym Sci*. 29 (2004) 699-766.
22. Y. Osada and D.E. De Rossi, *Polymer Sensors and Actuators, Springer,* Berlin (2010).
23. M.A. Rahman, P. Kumar, D.S. Park and Y.B. Shim, *Sensors* 8 (2008) 118-141.
24. U. Lange, N.V. Roznyatovskaya and V.M. Mirsky, *Anal Chim Acta* 614 (2008) 1-26.
25. Y. Li, B. Ying, L. Hong and M. Yang, *Synth Met*. 160 (2010) 455-461.
26. A.T. Ramaprasad and V. Rao, *Sens Actuators B Chem*. 148 (2010) 117-125.

27. N. Parvatikar, S. Jain, C.M. Kanamadi, B.K. Chougule, S.V. Bhoraskar and M.V.N.A. Prasad, *J. Appl Polym Sci.* 103 (2007) 653-658.
28. Y. Li, C. Deng, M. Yang, *Sens Actuators B Chem.* 165 (2012) 7-12.
29. S.K. Shukla, S.K. Shukla, P.P. Govender, E.S. Agorku, *Microchim. Acta* 183 (2016) 573-580.
30. C.W. Lin, Y.L. Liu and R. Thangamuthu, *Sens Actuators B Chem*. 94 (2003) 36-45.
31. M.M. Ayad, G. El-Hefnawey and N.L. Torad, *Sens Actuators B Chem*. 134 (2008) 887-894.
32. Y. Li, M.J. Yang, G. Casalbore-Miceli and N. Camaioni, *Synth. Met*. 128 (2002) 293-298.
33. H. Cankurtaran, O. Yazici, S. Dinc, F. Karaman, *Int. J. Electrochem. Sci.,* 8 (2013) 3265- 3278.
34. S. Dinç Zor, H. Cankurtaran *Journal of Sensors* (2016) Article ID 5479092.
35. A. Macagnano, E. Sgreccia, E. Zampetti, S. Pantalei, C. Di Natale, R. Paolesse, A. D'Amico, *Sens Actuators B Chem*. 130 (2008) 411–417.
36. K.P. Lee, A.I. Gopalan, S.H. Lee, A. Md. Showkat, Y.C. Nho, *J Appl Polym Sci*., 102 (2006) 3912–3918.
37. N.S. Afsharimani, A.I. Zad, M.J. Tafreshi, S. Salartayefeh, *J Appl Polym Sci*. 115 (2010) 3716–3720.
38. C. Steinem, A. Janshoff, Piezoelectric sensors, Springer, Berlin, 2006.
39. S.K. Vashist, P. Vashist, *Journal of Sensors* (2011) Article ID 571405.
40. G.Z. Sauerbrey, *Phys Journal* 155 (1959) 206-212.
41. R. Lucklum, C. Behling, P. Hauptmann, *Sens Actuators B Chem*. 65 (2000) 277–283.
42. C.D. Bain, G.M. Whitesides, *Science* 240 4848 (1988) 62-63.
43. Z. Wang, C.L. Chang, X. Zhao, W. Qian, X. Zhang, Z. Xie, B.H. Hwang, C. Hu, J. Shen, R.Hui, *J. Power Sources* 190 (2009) 351-355.
44. K.P. Biju, M.K Jain, *Meas Sci Technol*. 18 (2007) 2991–2996.
45. S. Korposh, R. Selyanchyn, S.W. Lee, *Sens Actuators B Chem*. 147 (2010) 599-606.
46. M.S. Gong, J.U. Kim, J.G. Kim, *Sens Actuators B Chem*. 147 (2010) 539-547.
47. T.M. Aminabhavi, H.T.S. Phayde*, Polymer* 36 (1995) 1023-1033.
48. M. Kikuchi, S. Shiratori, *Sens Actuators B Chem*. 108 (2005) 564–571.